Shap. Mem. Superelasticity (2018) 4:26–40
https://doi.org/10.1007/s40830-018-0161-4

SPECIAL ISSUE: A TRIBUTE TO PROF. JAN VAN HUMBEECK – A LIFETIME OF CONTRIBUTIONS TO UNDERSTANDING MARTENSITE, INVITED REVIEW PAPER

Frontiers of Theoretical Research on Shape Memory Alloys: A General Overview

Piyas Chowdhury[1]

Published online: 8 March 2018

Abstract In this concise review, general aspects of modeling shape memory alloys (SMAs) are recounted. Different approaches are discussed under four general categories, namely, (a) macro-phenomenological, (b) micromechanical, (c) molecular dynamics, and (d) first principles models. Macro-phenomenological theories, stemming from empirical formulations depicting continuum elastic, plastic, and phase transformation, are primarily of engineering interest, whereby the performance of SMA-made components is investigated. Micromechanical endeavors are generally geared towards understanding microstructural phenomena within continuum mechanics such as the accommodation of straining due to phase change as well as role of precipitates. By contrast, molecular dynamics, being a more recently emerging computational technique, concerns attributes of discrete lattice structures, and thus captures SMA deformation mechanism by means of empirically reconstructing interatomic bonding forces. Finally, ab initio theories utilize quantum mechanical framework to peek into atomistic foundation of deformation, and can pave the way for studying the role of solid-sate effects. With specific examples, this paper provides concise descriptions of each category along with their relative merits and emphases.

Keywords Shape memory alloy · Molecular dynamics · Density functional theory · Constitutive model · Micromechanical model

✉ Piyas Chowdhury
chowdhu2@illinois.edu

[1] Department of Mechanical Science and Engineering, University of Illinois at Urbana-Champaign, 1206 W. Green St, Urbana, IL 61801, USA

Introduction

Shape memory alloys (SMA), having remarkable multifunctional capabilities, find diverse applications in a broad spectrum of technological sectors e.g., biomedical, aerospace, automotive [1–3]. The most attractive feature of these alloys is their remarkable deformation recoverability achievable by simply regulating applied thermomechanical or magnetic stimuli. There exists a mounting need today for even superior SMAs, the quest for which is also undergoing rapid expansion. In these pursuits, theoretical research has played crucial roles by providing useful predictions on: (a) actuation performance of components (as described by pre-defined constitutive laws) [4, 5], (b) microscopic deformation mechanics and mechanisms (exploring the roles of reversible phase transformation, precipitation, internal twinning, slipping etc. and their mutual interactions) [6–8], and (c) discrete lattice physics (stemming from subtle quantum effects) [9, 10]. Individual avenues necessitate rigorous mathematical treatments and computations at multiple lengthscales ranging from continuum to sub-atomistics. Presently, there is no single predictive framework, which can uniformly incorporate multiscale physical phenomena of SMA deformations due to the immense complexity therein; rather, they are treated through independent modeling approaches. These theoretical endeavors, noticeably demarcated lengthscale-wise, are distinct in terms of governing principles, modeling emphases and core assumptions. This paper presents an overview on various theoretical frontiers by categorizing them as (a) macro-phenomenological, (b) micromechanical, (c) molecular dynamics, and (d) ab-intio models.

The extent of theoretical research on SMAs can be best understood with a panoramic perspective on materials structure hierarchy as in Fig. 1(a), which also juxtaposes

the scopes of existing experimental techniques. At the largest scale, simulations of actuation capability for various SMA-made components (e.g., a cardiovascular stent) are conducted for optimization purpose. Typically, finite element analyses are performed to investigate macroscale attributes such as stress/strain/temperature correlations, fracture and fatigue properties [6, 11]. Phenomenological formulations of phase transformation, metal plasticity, and thermodynamics constitute the governing principles of these simulations [12–15]. Alloy-specific constants needed for accurate modeling (e.g., transformation stress, strain, Young's moduli, thermal expansion coefficients) are typically obtained from empirical studies. The advantage of such approaches is that they can prove very useful optimization tools from applications standpoint, and can substantially reduce costs associated with trial-and-errors in laboratory experiments. One downside, however, is the non-consideration of microscopic deformation phenomena underlying macroscale responses. To that end, the microstructural deformation processes are modeled within the framework of Eshelby's micromechanical assumptions [7]. The micromechanical models allow theorization of phenomena at the single grain level such as compatibility of transformed domains embedded in parent phase, precipitate-induced elastic disturbances, and twinning-induced strain accommodations. Per the micromechanics theory, the grain-level deformation phenomena (e.g., evolving transformed domains, internal twins, precipitates) are modeled as continuum defects, which generate elastic disturbance fields [16]. Predictions from such models are typically validated with experimental characterization techniques, namely, electron microscopy, electron backscatter diffraction, X ray diffraction. Contrary to continuum-based phenomenological and micromechanical models, the evolution of phases at the nanoscale are simulated using atomistic methods such as molecular dynamics (MD) and density functional theory (DFT) [9, 10]. At the smallest spatial resolution (i.e., involving tens of atoms), the principal question of interest is how the electronic structure evolves subjected to alloying, and thus regulates the lattice energetics. Discrete lattice effects are essentially non-trivial, in that atomic ordering/stacking, d-orbital occupancy of constituent transition metals, etc. are major regulators of phase transformation propensity [17–20]. Common problems to be addressed from the angstrom level include the stability of phases, transformation energy pathways, elastic moduli, magnetism, defect energetics etc. Quantum mechanics based DFT simulation tools are employed to address these ultra-small scale issues, which are beyond the scope of any experimental characterization technique. Figure 1b presents a schematic timeline of all these modeling aspects. It follows that since the discovery of SMA in 1930s, theoretical research remained meager to non-existent [21]. After the hiatus of WW II, NiTi was discovered and studied with renewed interests. The scope of the literature especially on the continuum frontiers has been expanding over the past half a century. The arrival of MD models occurred in the last decade.

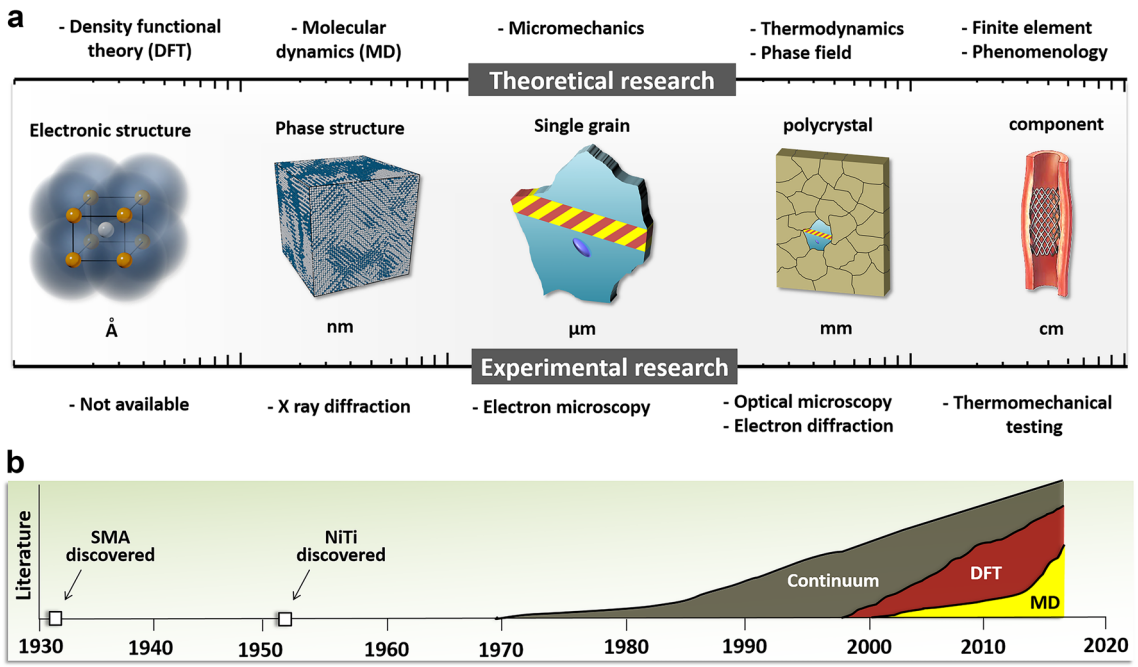

Fig. 1 **a** Experimental and theoretical research on shape memory alloys across multiple lengthscales, **b** a timeline of theoretical research classified into three broad categories, namely, continuum, DFT and MD (see text for discussions)

Compared to the DFT, the extent of MD literature is small due principally to the challenging task of developing an accurate empirical potential. However, most recent years are seeing a considerable emergence of new MD potentials for SMA materials, raising the extent of scientific publications.

A Brief Overview of General SMA Characteristics

Before describing the models, it would be instructive to briefly delineate the empirically known properties of SMAs and the associated microstructural evolution as in Fig. 2. Generally, three primary thermomechanical behaviors of SMAs are noted: (a) shape memory effect, (b) superelasticity and (c) isobaric shape memory effect.

The shape memory effect is the complete restoration of inelastic mechanical strains as a result of unloading, heating and cooling. Below M_f, the twinned martensite under stress becomes detwinned, which remains so after unloading. Heating of the stress-free detwinned martensite above A_f transforms it into an austenite, which upon cooling recovers the original twinned martensite structure. This is the so-called shape memory effect. Superelasticity or pseudoelasticity is the complete recovery of inelastic strain (as induced by phase transformation under stress) by merely removing the applied stress under isothermal condition above A_f. During superelastic loading/unloading, the austenitic phase transforms into a twinned martensite, which reverts back to the parent phase upon unloading. A temperature cycling at a constant stress, where the induced strain is recoverable, constitutes the isobaric shape memory behavior. Cooling below M_f induces twinning of martensite (from the original austenite) with an associated strain, which can be recovered by heating above A_f. As discussed next, each of the four categories of the modeling approaches attempts to address different aspects of these behaviors of SMAs.

Macro-phenomenological Models

In the SMA context, the constitutive modeling based on the macroscale phenomenology has remained a long-standing approach. These theories in many regards are similar to classical plasticity models [22]. For instance, they are geared primarily towards modeling the empirical mechanics and thermodynamics of deformation [16, 23, 24] by means of seeking solutions to continuum boundary-value problems. The emphasis is on developing ad hoc equations able to reproduce material-specific experimental stress/strain/temperature correlations. In doing so, both phase transformation- and plasticity-controlled thermomechanical constitutive responses are theorized [25]. However, the physics of microscopic deformation processes are not considered in developing these equations; rather, laboratory-measured uniaxial constitutive data remain the primary basis for model development. Thus, their predictive capability is contingent upon various empirically obtained materials constants e.g., Young's (or shear) modulus, transformation stress or strain, plastic yielding stress. The objective of the macro-phenomenological models is to provide general constitutive laws, which can eventually assist in component performance simulations [12, 26–29]. The scope of these models is wide, ranging from uniaxial tension–compression asymmetry to multi-axial non-proportional loading

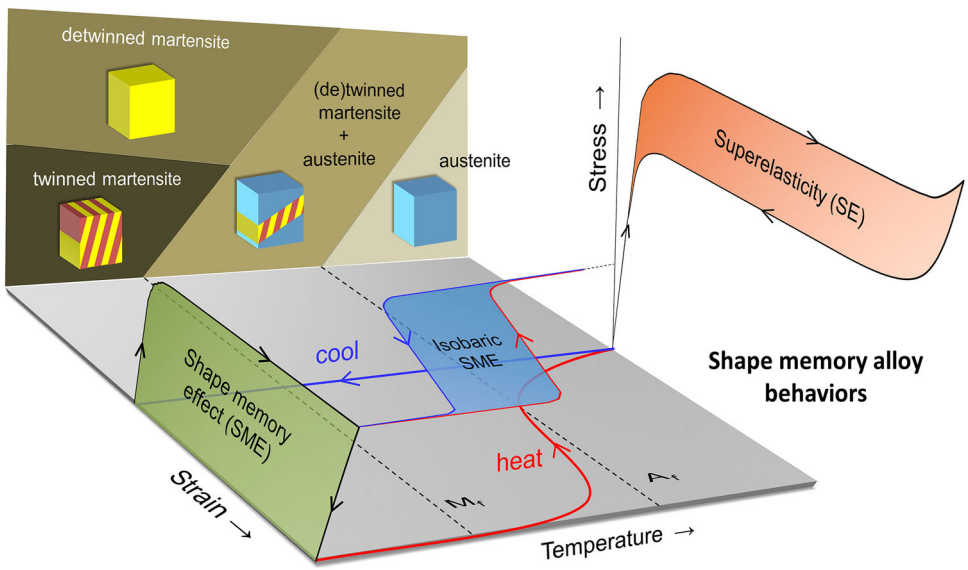

Fig. 2 Various thermomechanical responses of a generic shape memory alloy. The three major attributes that the SMAs typically demonstrate as actuators are: shape memory effects (SME), superelasticity (or pseudoelasticity) and isobaric SME. Underlying all these behaviors are complex microstructure changes involving reversible martensitic phase transformations and twinning/detwinning processes. See text for detailed discussions

scenario. Let us consider several case studies (as follows) to highlight the details of such modeling approach.

Several examples of numerical simulations of SMA-made actuators based on macro-phenomenological governing rules are presented in Fig. 3a–d. In Fig. 3a, a finite element simulation of a four-coil helical spring calibrated with NiTi properties is presented (adapted from [11]). This type of actuator is useful in automotive industries. In this boundary-value problem, the spring is subjected to axial end-forces. Based on the simulations [30], this study reports a marked non-homogeneities of stress distribution. Specifically, the effective stress was found to be most concentrated on the inner periphery of the spring, where damage is most likely to initiate during actual operation.

Similar simulations can be employed to determine the optimal geometry of, for example, a bone-implant assembly, whose function is to impart perfect cushioning of fractured bones. For instance, Fig. 3b presents a case study [31] where two NiTi plates are implanted on the bone with screws in the proximity of human humeral head (front and back). By imposing simulated movement of the bone, the displacement and the stresses both in the bone and the plates are studied. The governing laws relating the displacements and the stresses are based on the theories of simple linear elasticity, phenomenological phase transformation and plasticity. One can see the usefulness of such simulations as critical optimization tools, which can help circumvent costs and dangers of in vivo performance testing.

Figure 3c shows the finite element simulation of a cardiovascular stent [32] using material parameters corresponding to NiTi SMA. Such a device is inserted into a coronary artery in crimped form, and then is allowed to expand. Consequently, it assists in the flow of blood. The controlling constitutive laws in the simulations consider incremental energy minimization, where the total energy contribution is the sum of Helmholtz free energy and the deformation rate-independent dissipated energy. In the simulation of the stent as presented, it is crimped circumferentially. The distribution of martensite is then visualized. Notice that the maximum volume fraction of martensite (which is stress-induced) occurs at the bends. The superelastic stress–strain response, the tension–compression asymmetry as well as the materials anisotropy effects were also captured in these simulations.

One important application of a SMA-made actuator is the usage of chevrons in commercial jet engines for noise reduction purpose. A chevron is a serrated aerodynamic shape placed at the trailing end of the jet engine exhaust nozzle as in Fig. 3d. Based on actual test data by Boeing, Hartl, Lagoudas and co-workers [4, 5] examined (via a finite element model) the performance of three Ni60Ti40-made beams attached to a chevron. Using this 3D model, the nature of the chevron deflection under thermomechanical loading was investigated.

From the representative case studies described above, it seems that the combination of the finite element framework and the empirically based macro-phenomenological

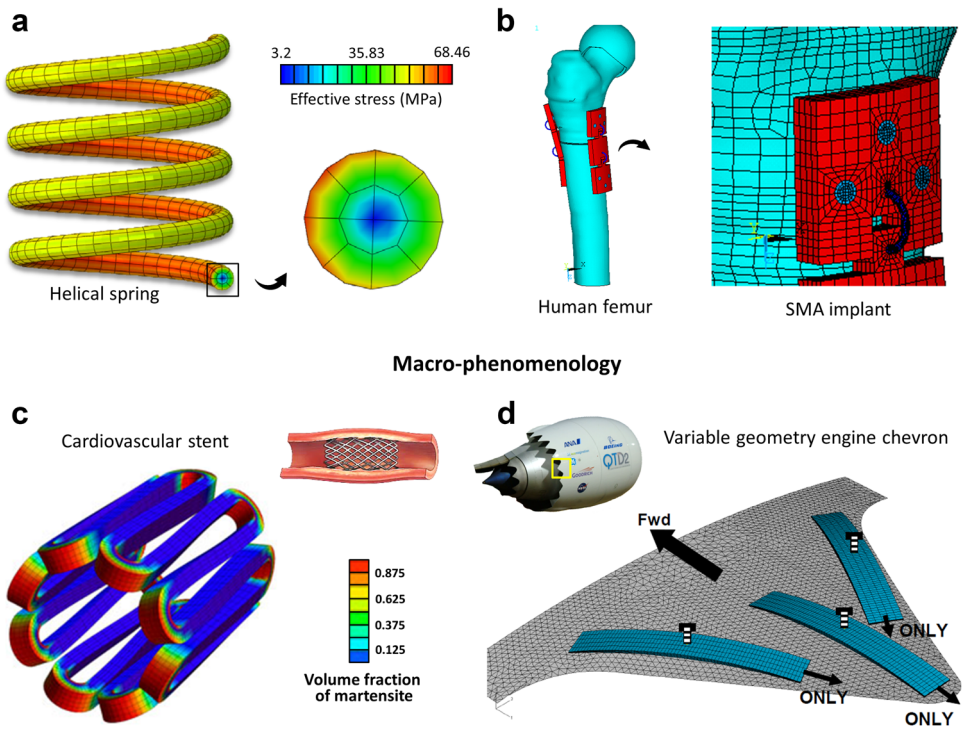

Fig. 3 **a** Finite element simulation of a four-coil helical spring based on NiTi properties [11], **b** the simulation of two NiTi plates implanted on a human bone with screws in the proximity of humeral head (front and back) [31], **c** finite element simulation of a cardiovascular stent [32] using material parameters corresponding to NiTi, and **d** finite element simulation of an aircraft engine chevron being investigated for deformation under operating thermomechanical load cycling [4, 5]. See text for detailed discussions

models is very useful for application optimizations. The alternative is to conduct many experimental trial-and-errors, which would be undoubtedly more expensive and would require rigorous resources. However, there is one important caveat in applying these models generically. Since the macroscale relationships are not based on the actual microscopic physics of deformation, the grain and/or sub-grain level phenomena, which can give rise to unexpected deformation trends, remain unexplored. For instance, the embedding of precipitates in the parent austenite would create long-range elastic straining, which would considerably modify the local deformation behavior. The macroscale properties would also be ultimately affected. The complex interaction among various defects e.g., localized slip, grain/twin boundaries would give rise to local weak points susceptible to cracking. Unless the model is explicitly trained to account for these microscopic processes, the merit of the phenomenological predictions could be interpreted qualitatively at best. To enhance the capability of phenomenological continuum-based laws, the micromechanical models are developed.

Micromechanics-Based Models

The purpose of micromechanics is related with determining the interplay of stress or strain at the lengthscale of materials microstructure [6, 13, 33–37]. The presence of multitudes of "defects" (e.g., transformed martensitic domains or precipitates embedded in the parent material, grain or twin boundaries) gives rise to a complicated network of overlapping deformation gradient fields. The primary purpose of micromechanical models in the SMA research context is to connect these microscopic intricacies of deformation with the global constitutive responses. Although the phase transformations fundamentally stem from atomic rearrangements of the parent lattice, the micromechanical models postulate the deformation scenario to be a continuum problem. This assumption is advantageous, in that the predictions of functional response are accomplished in a computationally feasible manner. The micromechanics is primarily based upon the Hookean relation between stress and strain tensors for infinite and continuous material as well as boundary values for semi-infinite ones. The presence of each defect is postulated as a source of "disturbance" in an otherwise infinitely extending continuum field. The solutions of the associated formulations are typically sought either analytically (i.e., in terms of closed-formed expressions) or numerically. The calibration of such models is strongly contingent upon empirically obtained various materials attributes at the mesoscale (e.g., texture, grain size, precipitate volume fraction), which are incorporated into the model so as to fine-tune the predictions.

Eshelby's Inclusion and Inhomogeneity Problems

The concept of the so-called "inclusion" or "inhomogeneity" by Eshelby [38] has remained one of the widely researched approach of describing the microscopic deformation processes in mathematical terms. To define them simplistically, an inclusion is a "foreign" particle embedded in the matrix material, which creates a so-called eigenstrain surrounding it. On the other hand, an inhomogeneity is a region of the material which has different elastic resistance to deformation (i.e., moduli) compared to the parent phase. The presence of either type of particle would create long-range elastic disturbance field as indicated schematically in Fig. 4a. However, the intensity of the fields is highest near the surface of these defects. Based on this simple definition, detailed mathematical formulations are devised to account for the stress–strain relations of the material (both single and polycrystals) [7]. The objective of the micromechanical concept is to capture the nuances of the SMA microstructure. In particular, the martensitic phase transformation is modeled in the form of embedded domains in a parent continuum field. The martensite forms local structures characterized by deformation twinning throughout the material. As these domains grow in volume, their mutual interaction as well as interplay with other pre-existent defects (e.g., grain boundaries) would essentially control the overall hardening behavior.

Precipitates in SMA Microstructure

Experimentally, the presence of non-transforming phase (in the form of precipitates) has been associated with beneficial effects (e.g., reduced hysteresis and transformation strain) on the mechanical attributes of many SMAs [39–42]. The presence of a precipitate in the microstructure creates local elastic disturbance, which could overlap with other precipitates, eventually creating an intricate network of strain fields. These fields largely influence the local preference of variant formation. Since the process of twin nucleation is essentially uni-directional in nature, the disturbance fields would bias the local resolved shear stress [42], thus helping nucleate a preferred variant over the other available systems. By utilizing the Eshelby's micromechanical formulations, Gall, Sehitoglu and co-workers [43] examined the distribution of the local resolved shear stress around a single coherent precipitate (Ni_4Ti_3) in NiTi matrix. The results are shown in Fig. 4b. From these calculations, one can see that the stress is highest in the close vicinity of the precipitate and begins to subside away from it. High-resolution transmission

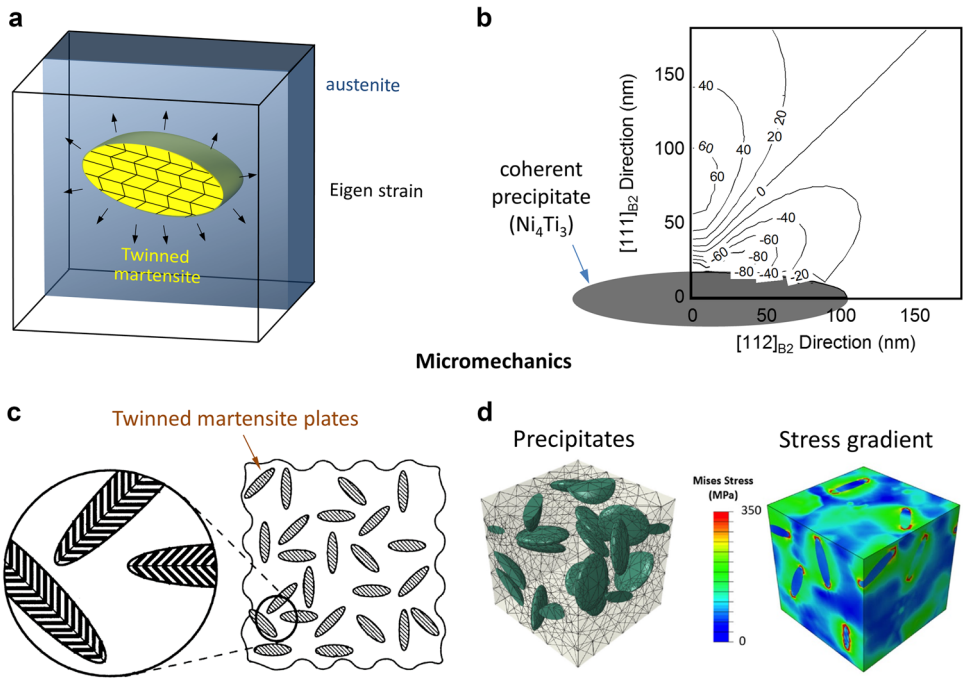

Fig. 4 **a** Per Eshelby's micromechanical theory [7], the presence of martensite in austenite matrix creates an eigen-strain, **b** the distribution of the local resolved shear stress around a single coherent precipitate (Ni_4Ti_3) in NiTi matrix [43], **c** the presence of the multiple variants consisting of internally twinned self-accommodated structures as envisioned by Huang and Brinson [6], and **d** a representative volume element (RVE) containing a distribution of Ni-rich precipitates in a discrete finite element domain [49, 50]

electron microscopy has indicated that the precipitates are usually rather tightly spaced [44, 45]. Thus, these stress contours would be overlapping.

Martensite Embedded in Parent Austenite

In addition to examining the effects on non-transforming precipitates, the prediction of SMA deformation behavior can also be performed by accounting for the micromechanics of phase transformation. Early endeavors [14, 46, 47] established the primary basis for modeling as the estimation of the collective interaction energies of the embedded domains. Patoor proposed a simplified interaction energy formulation by circumventing the use of Eshelby-type approach. Single- to poly-crystal transition was achieved by an averaging scheme. One similar example is provided in Fig. 4c after Huang and Brinson [6] to illustrate the concept. The presence of the multiple variants (consisting of internally twinned self-accommodated structure) is noted in the model. In this generic multivariant model, principles of thermodynamics and micromechanics are incorporated. The microstructure is modeled as having multiple martensite plates embedded in the austenite. Crystallographic input such as the habit planes and transformation and/or twinning directions are used to describe the local nature of deformation in a single grain under thermomechanical loads. Due to the combination of both micromechanics and thermodynamics, this model could capture the effects of general thermomechanical stimuli. Subsequently, they extended the model to study polycrystalline aggregates as well [48].

Physics of Precipitation: Role of Concentration Gradient

One important aspect of precipitation in the SMA microstructure is the depletion of one element type from the matrix as atoms diffuse to the precipitate during the aging treatment. The effects of both element concentration gradient and elastic disturbance fields in fact play a role in deciding the overall alloy mechanical properties. Most recently, Baxevanis, Lagoudas, and co-workers forwarded a model in this regard [49, 50], which can be applicable to several SMA materials (e.g., NiTi, NiTiHf) [51]. In Fig. 4d, the typical representative volume element (RVE) containing a distribution of oblate Ni-rich precipitates in a discretized finite element domain is shown. In the right inset, the simulation results demonstrating the Von Mises stress distribution throughout the RVE can be seen. Notice a higher stress concentration in the very close vicinity of the precipitates surfaces. The materials input for the predictions were obtained from experiments. By accounting for micromechanics and the chemical effects (e.g., Ni depletion from the matrix), a good agreement between the predictions and the experimental findings was established.

Molecular Dynamics (MD) Models

Compared to the large volume of literature on other modeling avenues, molecular dynamics-based studies of SMAs are considerably limited, centering mostly on NiTi. Some recent studies on Ni–Al–Co have emerged [52, 53]. This

scarcity is attributed to the lack of material-specific accurate "potentials" that can faithfully capture multiple stable phases and their reversibility. In the MD context, a potential is a pre-determined database of interatomic bonding energy landscape, which obviates the need for solving computationally expensive sets of many-body Schrodinger's equations [54]. Earliest endeavors on MD simulations are initiated with Farkas et al.'s [55] proposition of an EAM potential i.e., embedded atom method [56, 57]. An EAM potential theorizes the energetic expenditure for individual pair-wise interactions and for embedding atoms in an overlapping electronic cloud. They aimed at capturing only B2 phase properties. By considering generic pair-wise interaction among metallic atoms (in the form of Lennard-Jones potential [58]), Kastner and co-workers investigated SME and the associated evolution of the austenite phase into martensite [59–61]. Subsequently, Lai and Liu developed an EAM potential [62, 63] for predicting solid solubilities of amorphous (i.e., disordered) Ni–Ti intermetallics. Lai and Liu's potential spawned several improved adaptations, most notable among which are those by Mutter and Nielaba [64, 65], and Zhong et al. [66–69]. Most recently, another EAM potential by Ren and Sehitoglu has also been reported [70].

To capture effects of covalent bonding, the EAM formalism can be further modified by incorporating the directional nature of interatomic interactions for the many-body problem [71–73]. Earlier, Ishida and Hiwatari [74] was able to employ modified EAM (MEAM) methodology to capture thermally induced and reversible B2 $\leftrightarrow$ B19′ transformations. More recently, Ko et al. [75] proposed an improved MEAM potential which can predict reversible phase transformation underlying both single- and polycrystalline deformation.

Shape Memory Effect (SME)

Figure 5a presents an MD case study [76] of shape memory effect (SME) of NiTi by Mutter and Nielaba who adapted the original Lai and Liu's potential by introducing smooth cut-off behavior [64, 65]. A multi-variant B19′ (indicated by light and dark brown regions) is strained up to about 10% and then unloaded. In the process, one variant undergoes progressive growth by detwinning process at the expense of others. The unloading followed by heating leads to the reversal of the process. As a result, a twinned (i.e., multi-variant) martensite is formed along with the full recovery of strain. Mutter and Nielaba attributed the absence of B2 austenite phase (which is unlike the experimental findings) to a smaller energy barrier for twinning (during heating of the unloaded single variant) than the B19′-to-B2 transformation. This behavior might be subjected to modification depending on the potential. For the case of the adapted Lai and Liu's potential by Zhong et al. [68, 69], the SME of NiTi has been associated with B2 → B19 → BCO → twinned BCO transformation, which was characterized by the formation of "macroscopic twin-like" deformation of the nanowire.

Superelasticity

Most literature on the MD-based studies on SMA superelasticity are centered on equiatomic binary NiTi [66–70, 75, 77, 78]. Zhong et al. [68, 69] reported that the superelastic response of NiTi nanowires at 400 K under compressive stress along the [011] direction stems from the reversibility of the forward transformation path: B2 → B19 → B19′. At lower temperature (350 K), the transformation steps are altered to: B2 → B19 → BCO → twinned BCO at 350 K (BCO being body-centered orthorhombic). It is worth recalling that the intermediate B19 phase has not been experimentally evidenced in the solutionized condition, rather only in aged NiTi (i.e., in the presence of precipitates) or when alloyed with Cu or Fe [79–81]. Similarly, the likelihood of the BCO phase, although not substantiated experimentally in NiTi, has been predicted by several research groups [82–86] from first principles. Combined empirical and simulation results pose interesting questions about the phase stabilization process in NiTi SMA. The occurrence of a certain phase in atomistic simulations would be favored by its energetic state as defined in the potential. Thus, it is possible that the transformation energy pathway in the pristine defect-free simulated lattice apparently may or may not contribute to the temporal and spatial stabilization of intermediate phases. For instance, in the MD models by Chowdhury et al. as well as by Ko et al. [75] B19 or BCO phases were not observed.

Only very recently, strain recovery properties of ternary Co–Ni–Al SMAs are investigated by Yamakov, Mishin and co-workers [52, 53] as in Fig. 5b. They proposed an MD model on the superelastic behavior of Co–Ni–Al-based SMAs. The high-temperature B2 austenite structure is created via Monte Carlo equilibration. The origin of the hysteresis is attributed to twinning followed by reversible detwinning processes. In their simulations, pseudoelastic stress–strain responses under tensile and compressive loads were found to differ significantly as two case studies on [110] and [001] crystallographic directions demonstrated. The structural changes associated with the recovery were traced to the reversible transformation between the parent B2 and the twinned $L1_o$ lattices. Interestingly, the magnitude of the stress plateau was found to be on the order of MPa, unlike typical MD simulations where GPa-level stresses are noted for uniaxial loading.

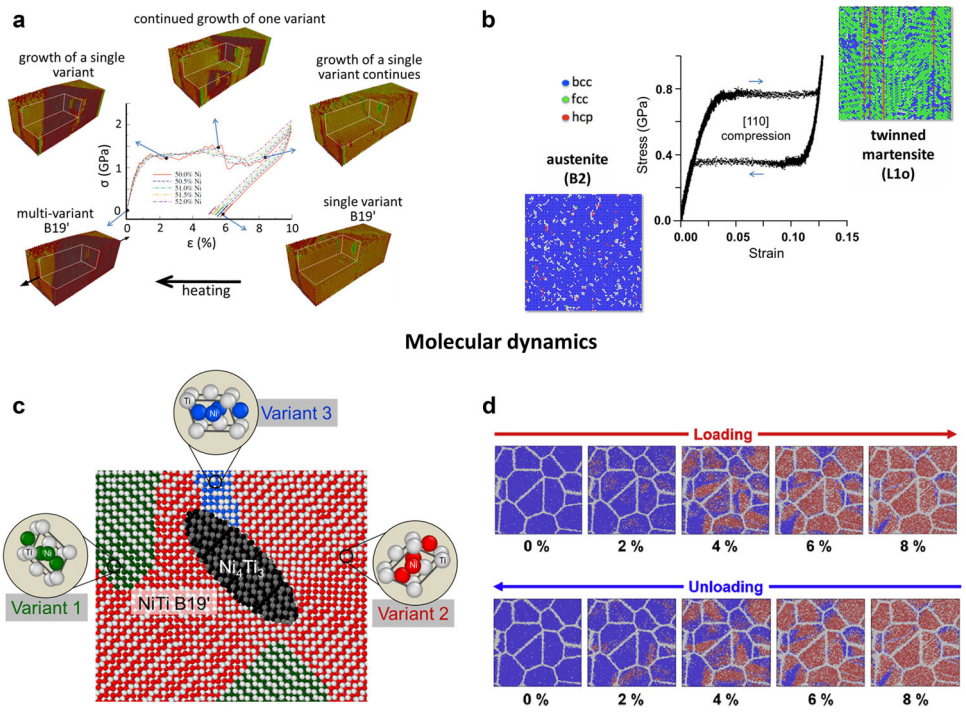

Fig. 5 **a** Stress–strain response of NiTi martensite demonstrating evolution of multi-variant martensite into a single variant and the reverse process upon heating [76], **b** MD simulations of superelastic strain recovery of single crystals Co–Ni–Al SMA [52, 53] undergoing reversible transformation between B2 austenite and $L1_o$ martensite, **c** the presence of a nano-sized coherent precipitate in austenitic NiTi matrix [87] causing activation of different variants while setting preference for a certain variant, and **d** reversible martensitic transformation in nanocrystalline NiTi under uniaxial tension at 400 K (blue regions corresponding to austenite while red to martensite) [78]

Presence of Non-transforming Phase

MD studies have uncovered important mechanistic insight into how a single nano-sized precipitate can affect the deformation properties [87, 88]. Earlier, Sato et al. [88] modeled a single plate-shaped precipitate (embedded in B2 NiTi) to be of body-centered tetragonal (bct) symmetry. They noted the following observations: (i) a modification of the potential energy landscape at the interface, which extends inside the precipitate lattice, and (ii) the presence of the particle results in the reduction of applied tensile stress. Furthermore, the interfacial mismatch was associated with a preferred sited for martensite nucleation. However, experimental studies noted that the precipitates in NiTi are of rhombohedral lattice (Ni_4Ti_3) and of lenticular geometry [89–91]. Chowdhury et al. [87] studied the effects of a lenticular Ni_4Ti_3 precipitate on the phase transformation propensity as well as the associated constitutive characteristics. They predicted a stress gradient field surrounding the precipitate, which they attributed to the inter-lattice misfit between the rhombohedral and the surrounding B2 matrix. The presence of the stress gradient was found to influence the variant nucleation preference. As in Fig. 5c, one variant (designated "variant 3") is preferred over the rest, a phenomenon evidenced through electron microscopy earlier [92]. The MD study also implied that the nano-precipitate serves to reduce transformation stress, hysteresis, and transformation strain.

Polycrystallinity: Role of Grain Boundaries

The aforementioned studies considered a single grain setting for modeling. In most applications, the SMAs are used in their polycrystalline microstructure. The modeling of polycrystalline microstructure is of particular interest from a practical engineering standpoint. In Fig. 5d, atomic configuration of nanocrystalline NiTi (average grain diameter being 20 nm) under tensile loading/unloading cycle at 400 K is presented after Ko et al. [78]. In this simulation, the austenite began to transform into martensite in the bulk of the grains away from the grain boundaries. As the loading progressed, the martensite phase was observed to expand towards the interface. By contrast, during unloading, the martensite-to-austenite transformation began at the boundaries, which then propagated inside the grain interiors.

Density Functional Theory-Based Models

Important discoveries made from ab initio simulations include determination of transformation energy pathway, elastic moduli, phase stability [82, 84, 85] etc. as a direct consequence of the electronic structure. The sub-lattice effects are addressed by solving many-body Schrodinger's equation with a view to iteratively seeking the energetic ground state of the overall crystal. To reduce computational loads, Born–Oppenheimer approximations are adopted, which dictates instantaneous and simultaneous

updating of atomic nucleus and the orbiting electron cloud. This essentially obviates the time-dependency of wave functions (which represent electrons) from Schrodinger's equation. Furthermore, instead of wave functions, the temporal and spatial trajectories of individual valence electrons are solved in terms of "charge densities." The total potential energy of, say, a prototypical-simulated lattice is a function of charge distribution. Other important variables directly affecting evolution of electronic cloud are, namely, the quantized nature of lattice vibrations (i.e., phonons), electron spin orientation (i.e., magnetism). By accounting for these discrete lattice effects, new clarifications on deformation propensity have emerged (discussed next).

Magnetic Attributes of SMAs

Ferromagnetic SMAs such as Ni_2MnGa, Ni_2FeGa possess unique shape-recovering capability, which is magnetically induced. The austenite phase is an ordered face-centered cubic lattice ($L2_1$) [93, 94], and the martensite can be tetragonal or orthorhombic (with the possibility of modulated structures) [95–97]. The shape recovery mechanism involves the realignment of inherent magnetic domains, which in turn generates mechanical driving force for two-way twinning/detwinning processes. The process is schematically shown in the right inset of Fig. 6a, where red and yellow regions represent two different variants in the martensitic phase [98]. In presence of an applied magnetic field (H), the magnetic moments of individual variants (indicated by arrows) would attempt to align with H, which in turn would initiate detwinning of one variant at the expense of another. The contour map on the left inset represents variation of energy as a function of magnetic moment and lattice tetragonality (i.e., *c*/*a* ratio) as predicted from first principles [18] for stoichiometric Ni–Mn–Ga SMA. Notice the location of absolute energy minimum at $c/a = 1$. It is noted that the material can reach another energy minimum at larger *c*/*a* without any change in the magnetic moment. These alloys are strong functions of compositions. In particular, addition of Mn can substantially modify local magnetic moment [17, 99].

Transformation Energy Pathways

The significance of transformation energetics is that they signify the relative energetic preference of all the phases encountered during the transformation. For instance, the energy pathway for NiTi has been studied by many independent groups [83–86]. It was discovered that B19′ is not the global energy ground state. A body-centered orthorhombic (BCO) structure, also known as the B33 phase, is energetically the most stable phase. It should be noted that the existence of B33 has never been experimentally substantiated. The rationale for stabilization of B19′, despite not being the global minima, is attributed to the presence of an energy barrier by some researchers [100, 101], which can be considerably enhanced due to the stress triaxiality in the microstructure [101]. No other research groups, however, discovered the presence of any energy barrier so far; more independent research is needed for confirmation. Another important SMA, whose transformation paths are studied extensively, is ferromagnetic Ni_2MnGa. In Fig. 6b, the structural energy as a function of tetragonality (*c*/*a* ratio) indicates a gradual decrease in the total energy due to martensitic transformation (from $L2_1$ austenite to $L1_o$ martensite). In addition, the modulated martensite structures i.e., 10 and 14 M (also known as "adaptive martensite") are of low energy structures without substantial change in *c*/*a* ratio from the austenite phase. These findings are consistent with experimental observations, where modulated phases are reported to be predominant in the martensitic phase [102, 103].

Elastic Moduli

One of the significant achievements of the first-principles models is the prediction of elastic moduli [19, 20, 85]. For instance, as shown schematically in Fig. 6c, a twinned martensite (single crystal) of NiTi SMA becomes fully detwinned into a single variant after considerable straining. The elastic stretching of twinned lattice dictates the slope of the loading curve. On the other hand, the unloading of fully detwinned martensite is controlled by the elastic moduli of a single-variant crystal. The two slopes (loading and unloading) essentially have different magnitudes due to the differences in the twinned and detwinned lattice structures. Wagner and Windl [19] calculated the stiffness constants of B19′ crystal, a 3D representation of which is shown in the inset of Fig. 6c. Sehitoglu and co-workers examined the moduli of twinned B19′ lattice of NiTi from first principles [10]. Notice that the twinned lattice has considerably smaller magnitude of directional moduli. For example, E_{100} and E_{001} of the twinned structure are one-third of the detwinned lattice. The results point to the role of reflective symmetry of lattice (i.e., via twinning) in reducing the resistance to elastic deformation. In another undertaking, Wagner and Windl [20] also predicted the moduli mismatch between a B2 NiTi and a rhombohedral Ni_4Ti_3 precipitate. They noted that the maximum modulus difference exits along the direction perpendicular to the precipitate equatorial plane i.e., E_{111}. Since the material always seeks to minimize its strain energy, this result implies that the precipitate forms with a flat lenticular shape and a circular cross section so as to reduce the overall elastic strain energy.

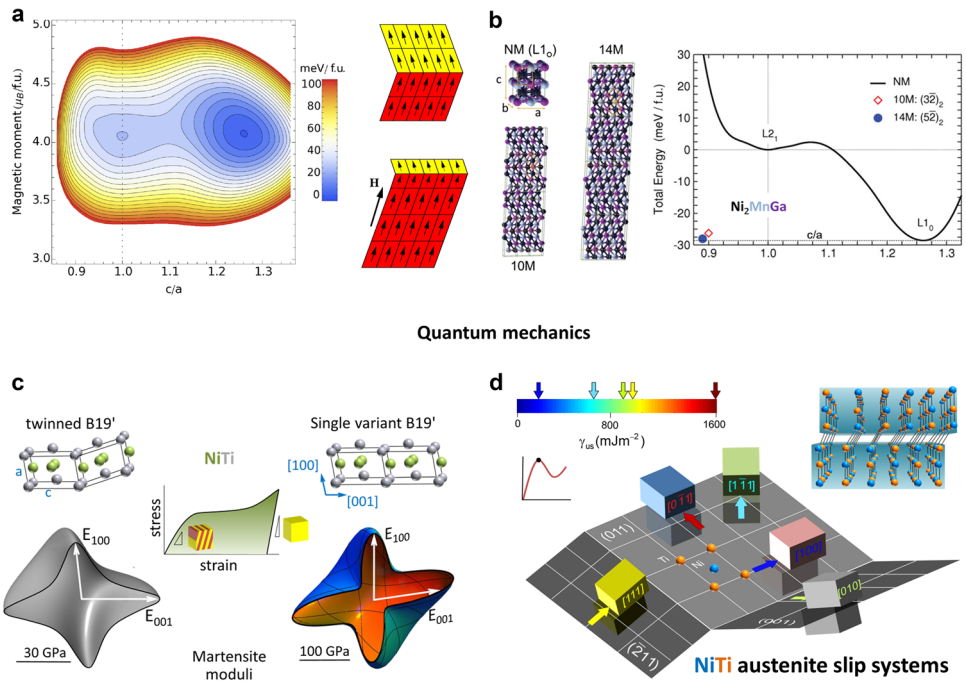

Fig. 6 **a** Contour map representing variation of energy as a function of magnetic moment and lattice tetragonality (i.e., *c*/*a* ratio) predicted from first principles [18] for stoichiometric Ni–Mn–Ga SMA. **b** different martensite crystal structures (non-modulated i.e., NM, modulated 10 and 14 M) ([127]) and the structural energy as a function of tetragonality (*c*/*a* ratio) [127, 128]. **c** stiffness moduli for a twinned B19′ lattice [10, 19] corresponding to slopes of elastic portions of loading/unloading curves, and **d** comparison of slip energy barrier (γ_{us}) computed by rigid-shear of lattice half-blocks for five different slip systems in NiTi austenite (B2) lattice [9, 100]

Energetics of Plastic Deformation

Plastic deformation in SMAs is the reason for their performance degradation. Although nominal plastic yield stress is much greater than the transformation stress in SMAs, considerable slip activities can accompany phase transformation processes microscopically [104–106]. Mesoscale factors such as preferential grain orientation (inducing maximum resolved shear stress on the slip systems), interfacial incompatibility between austenite and martensite etc. can facilitate plastic deformation. At the atomic lengthscale, slipping is essentially a form of permanent lattice shearing of the closest-pack plane, whose direction and magnitude are represented by the Burgers vector. By exploiting this simple yet intuitive definition, DFT calculations have provided a unique measure of comparing relative slipping strength of various systems. In Fig. 6d, the energy barriers (unstable stacking fault energy "γ_{us}", which is the peak on the energy-shear displacement curve) to activate five different possible slip systems in the austenite phase are compared [9, 100]. The following order of energy barriers is predicted:

$$\gamma_{us}^{(011)[0\bar{1}1]} > \gamma_{us}^{(001)[010]} > \gamma_{us}^{(\bar{2}11)[\bar{1}01]} > \gamma_{us}^{(011)[1\bar{1}1]} > \gamma_{us}^{(011)[001]},$$

which establishes the (011)[001] system as the most prone to slipping. On a physical ground, the most favorable slip system corresponds to the one with smallest nearest neighbor distance. Similar energetic comparison is also noted for the tetragonal martensite lattice of Ni_2FeGa SMAs. In addition to quantifying the relative slipping propensity of existing alloys, these results encourage further potential research directed at concocting new alloys with superior slip resistance.

Synergy or Unification of Multi Lengthscale Modeling Techniques

As the forgoing discussions imply, the fundamentals of continuum mechanics, thermodynamics, micromechanics, statistical mechanics, quantum mechanics are quite well established to address SMA deformation. While it is hypothetically possible to combine theories of multiscale physical phenomena, the major obstacle to actual implementation thereof is the processing ability of computers. While there are many commercial softwares available for finite element analysis, they are mostly founded on macroscale empirical laws of phase transformation and plasticity. The accuracy of these tools is as good as the underlying constitutive formulations as programmed. Today, a unification of various modeling approaches to accurately address practical engineering issues remains a highly coveted yet challenging task [107]. An ideal modeling goal would be to incorporate all the necessary physics of deformation across lengthscale and seek the macroscale solution, which inevitably invokes massive computational burden. Even with the arrival of exascale computing with modern clusters, the prospect of a massive unified modeling framework suitable for engineering purpose is not imminent. To address materials structural hierarchy, research efforts have been directed towards extracting

critical parameters from atomistics and incorporating them in continuum models. For instance, the classical Peierls–Nabarro framework has recently been revisited, whereby DFT-based energetics are utilized to predict critical stresses for slip, twinning etc. [108–110]. For phenomenological models, these critical stresses are important parameters, which are conventionally used on ad hoc basis.

The importance of bridging discrete lattice effects with continuum properties cannot be understated. To illustrate, empirical data (transformation temperature, recoverable strain and slip strength) for a range of SMAs is mapped, and compared with known atomistic data on slip resistance (in terms of normalized γ_{us}) in Fig. 7. The desired attributes in an SMA are: (i) low transformation stress so that reversible phase transformation is easily triggered, (ii) high slip resistance so that plastic deformation can be avoided, (iii) high recoverable strain for greater actuation capability, and (iv) low or high transformation temperature depending on application. Exhaustive sets of laboratory experiments are needed to properly map the materials property correlations such as in Fig. 7. Interestingly, the γ_{us} values (which is an indicator of slip resistance computed from first principles based on pristine single grain configuration) follow the same materials-specific trends observed empirically. The presence of such strong correlation highlights the need for further research into the utility of micro- and nanoscale simulations. It remains to be seen how atomistically informed parameters can benefit continuum-based models, a promising research arena that necessitates combined efforts of independent research groups.

Concluding Remarks

In this paper, we have highlighted the applicability and the primary emphases of various modeling techniques under the generalizations: (a) macro-phenomenological, (b) micromechanical, (c) molecular dynamics, and (d) ab-intio models. The modeling endeavors revolve around two broad objectives, namely, (i) the prediction of existing materials properties under various thermo-mechanical conditions, and (ii) the understanding of microscopic mechanisms towards designing new and novel materials. The former is more widely practiced than the latter, which nonetheless is coming of age as a powerful tool. Now, the logical question to ask is how one can utilize phenomena occurring at multiple physical lengthscales to address problems of more immediate necessity. For instance, one of the prominent real-life applicability concerns is the failure of materials (e.g., cracking), especially due to irreversible damage induced upon substantial operating cycles. Cyclic damage in the SMA context is generalized into [15, 111–115]: (a) functional fatigue and (b) structural fatigue. Functional fatigue is caused by the modification to superelastic responses over cycles, which results from persistent accumulation of slip and martensite. By contrast, structural fatigue refers to continuous cracking (as a result of

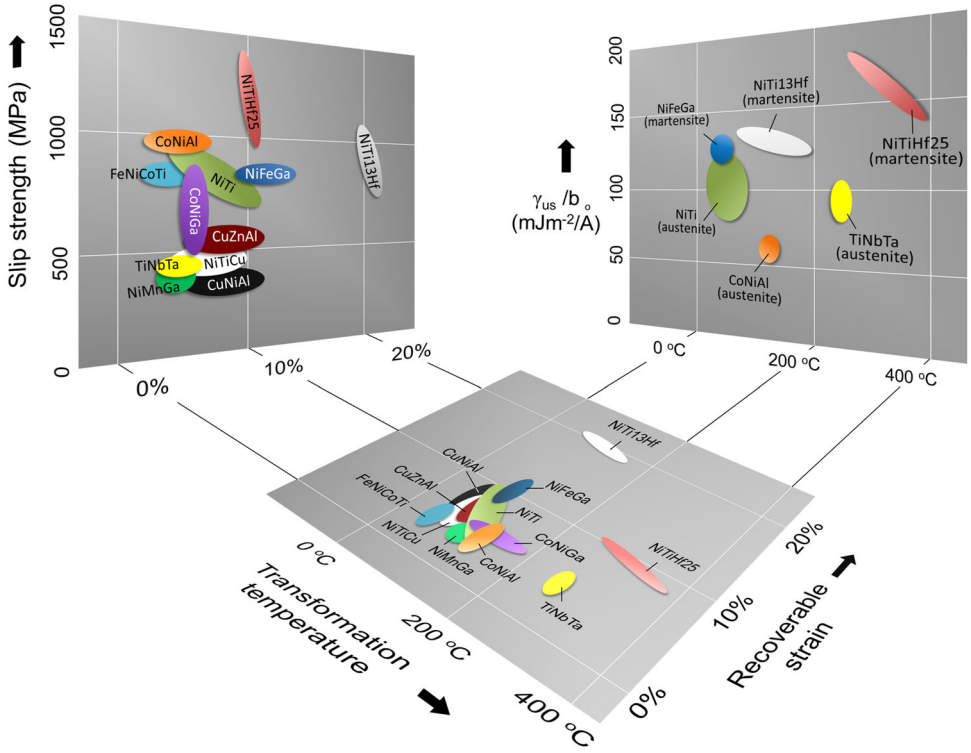

Fig. 7 Comparison of various shape memory alloys in terms of their experimentally determined transformation temperature (i.e., austenite finish temperature), recoverable strain (total strain minus elastic and plastic ones) and slip strength (marking the macroscale yielding of an SMA) juxtaposed with atomistically predicted slip resistance (normalized by Burgers vector magnitude, b) [9, 100]

localized plasticity and residual martensite) towards catastrophic fracture. Fatigue is of particular concern in aerospace structures for any type of material [116]. Given the rising utility of SMAs in aeronautical industries, the need for proper characterization as well as prediction of fatigue is critical. The literature on atomistic simulations on the topic of cracking mechanism at the nanoscale is emerging for conventional (i.e., non-transforming) materials [117–126, 129]. In order to retain strain recoverability i.e., the phase reversibility, it is desired to minimize slip activities in a SMA. Increased degree of slipping can adversely affect the reversibility of transformation. While the empirical approaches address the engineering properties, it remains to be seen how, with existing pace in developing new MD potentials as well as faster DFT simulations, SMA damage modeling could benefit therefrom.

Acknowledgements The author acknowledges the financial support from the department of mechanical science and engineering in University of Illinois at Urbana-Champaign (UIUC).

References

1. Jani JM, Leary M, Subic A, Gibson MA (2014) A review of shape memory alloy research, applications and opportunities. Mater Des 56:1078–1113
2. Duerig T, Pelton A, Stöckel D (1999) An overview of nitinol medical applications. Mater Sci Eng, A 273:149–160
3. Chowdhury P, Canadinc D, Sehitoglu H (2017) On deformation behavior of Fe-Mn based structural alloys. Mater Sci Eng 122:1–28
4. Hartl DJ, Lagoudas DC (2007) Characterization and 3-D modeling of Ni60Ti SMA for actuation of a variable geometry jet engine chevron. In: The 14th International symposium on: smart structures and materials & nondestructive evaluation and health monitoring. In: International society for optics and photonics, pp 65293Z-65293Z-65212
5. Oehler S, Hartl D, Lopez R, Malak R, Lagoudas D (2012) Design optimization and uncertainty analysis of SMA morphing structures. Smart Mater Struct 21(9):094016
6. Huang M, Brinson L (1998) A multivariant model for single crystal shape memory alloy behavior. J Mech Phys Solids 46(8):1379–1409
7. Mura T (2013) Micromechanics of defects in solids. Springer, New York, p 2013
8. Paranjape HM, Manchiraju S, Anderson PM (2016) A phase field–Finite element approach to model the interaction between phase transformations and plasticity in shape memory alloys. Int J Plast 80:1–18
9. Chowdhury P, Sehitoglu H (2017) A revisit to atomistic rationale for slip in shape memory alloys. Prog Mater Sci 85:1–42
10. Chowdhury P, Sehitoglu H (2017) Deformation physics of shape memory alloys–fundamentals at atomistic frontier. Prog Mater Sci 88:49–88
11. Saleeb A, Dhakal B, Hosseini M, Padula S II (2013) Large scale simulation of NiTi helical spring actuators under repeated thermomechanical cycles. Smart Mater Struct 22(9):094006
12. Lubliner J, Auricchio F (1996) Generalized plasticity and shape-memory alloys. Int J Solids Struct 33(7):991–1003
13. Patoor E, Eberhardt A, Berveiller M (1996) Micromechanical modelling of superelasticity in shape memory alloys. Le J de Physique IV 6(C1):C1-277
14. Raniecki B, Lexcellent C, Tanaka K (1992) Thermodynamic models of pseudoelastic behaviour of shape memory alloys. Arch Mech, Archiwum Mechaniki Stosowanej 44:261–284
15. Robertson S, Pelton A, Ritchie R (2012) Mechanical fatigue and fracture of Nitinol. Int Mater Rev 57(1):1–37
16. Brinson LC (1993) One-dimensional constitutive behavior of shape memory alloys: thermomechanical derivation with non-constant material functions and redefined martensite internal variable. J Intell Mater Syst Struct 4(2):229–242
17. Enkovaara J, Heczko O, Ayuela A, Nieminen RM (2003) Coexistence of ferromagnetic and antiferromagnetic order in Mn-doped Ni 2 MnGa. Phys Rev B 67(21):212405
18. Entel P, Buchelnikov V, Gruner ME, Hucht A, Khovailo VV, Nayak SK, Zayak AT (2008) Shape memory alloys: a summary of recent achievements. In: Materials science forum. Trans Tech Publ, pp 21–41
19. Wagner M-X, Windl W (2008) Lattice stability, elastic constants and macroscopic moduli of NiTi martensites from first principles. Acta Mater 56(20):6232–6245
20. Wagner MFX, Windl W (2009) Elastic anisotropy of Ni_4Ti_3 from first principles. Scripta Mater 60(4):207–210
21. Otsuka K, Wayman CM (1999) Shape memory materials. Cambridge University Press, Cambridge
22. Khan AS, Huang S (1995) Continuum theory of plasticity. Wiley, New York
23. Tanaka K, Nagaki S (1982) A thermomechanical description of materials with internal variables in the process of phase transitions. Arch Appl Mech 51(5):287–299
24. Liang C, Rogers CA (1997) One-dimensional thermomechanical constitutive relations for shape memory materials. J Intell Mater Syst Struct 8(4):285–302
25. Auricchio F, Reali A, Stefanelli U (2007) A three-dimensional model describing stress-induced solid phase transformation with permanent inelasticity. Int J Plast 23(2):207–226
26. Boyd JG, Lagoudas DC (1994) Thermomechanical response of shape memory composites. J Intell Mater Syst Struct 5(3):333–346
27. Birman V (1997) Review of mechanics of shape memory alloy structures. Appl Mech Rev 50:629–646
28. Pelton A, Schroeder V, Mitchell M, Gong X-Y, Barney M, Robertson S (2008) Fatigue and durability of Nitinol stents. J Mech Behav Biomed Mater 1(2):153–164
29. Lecce L (2014) Shape memory alloy engineering: for aerospace. Elsevier, Structural and Biomedical Applications
30. Saleeb A, Padula S, Kumar A (2011) A multi-axial, multi-mechanism based constitutive model for the comprehensive representation of the evolutionary response of SMAs under general thermomechanical loading conditions. Int J Plast 27(5):655–687
31. Tarnita D, Tarnita D, Bolcu D (2011) Orthopaedic modular implants based on shape memory alloys. INTECH Open Access Publisher, Vienna
32. Stupkiewicz S, Petryk H (2013) A robust model of pseudoelasticity in shape memory alloys. Int J Numer Meth Eng 93(7):747–769
33. Sun QP, Hwang KC (1993) Micromechanics modelling for the constitutive behavior of polycrystalline shape memory alloys—I. Derivation of general relations. J Mech Phys Solids 41(1):1–17
34. Goo B, Lexcellent C (1997) Micromechanics-based modeling of two-way memory effect of a single crystalline shape-memory alloy. Acta Mater 45(2):727–737

35. Gao X, Huang M, Brinson LC (2000) A multivariant micromechanical model for SMAs Part 1. Crystallographic issues for single crystal model. Int J Plast 16(10):1345–1369
36. Vivet A, Lexcellent C (1998) Micromechanical modelling for tension–compression pseudoelastic behavior of AuCd single crystals. Eur Phys J Appl Phys 4(2):125–132
37. Lu Z, Weng G (1997) Martensitic transformation and stress-strain relations of shape-memory alloys. J Mech Phys Solids 45(11–12):19051923–19211928
38. Eshelby JD (1957) The determination of the elastic field of an ellipsoidal inclusion, and related problems. In: Proceedings of the Royal Society of London A: mathematical, physical and engineering sciences, The Royal Society, pp 376–396
39. Tanaka Y, Himuro Y, Kainuma R, Sutou Y, Omori T, Ishida K (2010) Ferrous polycrystalline shape-memory alloy showing huge superelasticity. Science 327(5972):1488–1490
40. Chumlyakov YI, Kireeva I, Panchenko EY, Timofeeva EE, Kretinina I, Kuts O, Karaman I, Maier HJ (2017) Shape memory effect and superelasticity in single crystals of high-strength ferromagnetic alloys. In: Advanced materials research, Trans Tech Publ, pp 15–22
41. Ma J, Hornbuckle B, Karaman I, Thompson G, Luo Z, Chumlyakov Y (2013) The effect of nanoprecipitates on the superelastic properties of FeNiCoAlTa shape memory alloy single crystals. Acta Mater 61(9):3445–3455
42. Gall K, Sehitoglu H, Chumlyakov YI, Kireeva I (1999) Tension–compression asymmetry of the stress–strain response in aged single crystal and polycrystalline NiTi. Acta Mater 47(4):1203–1217
43. Gall K, Sehitoglu H, Chumlyakov YI, Kireeva IV, Maier HJ (1999) The influence of aging on critical transformation stress levels and martensite start temperatures in NiTi: part II—discussion of experimental results. J Eng Mater Technol 121(1):28–37
44. Schryvers D, Tirry W, Yang Z (2006) Measuring strain fields and concentration gradients around Ni_4Ti_3 precipitates. Mater Sci Eng, A 438:485–488
45. Tirry W, Schryvers D (2005) Quantitative determination of strain fields around Ni_4Ti_3 precipitates in NiTi. Acta Mater 53(4):1041–1049
46. Delaey L, Ortin J, Van Humbeeck J (1987) Hysteresis effects in martensitic non-ferrous alloys. In: Proceedings of the phase transformations'87, pp 60–66
47. Fischer F, Tanaka K (1992) A micromechanical model for the kinetics of martensitic transformation. Int J Solids Struct 29(14–15):1723–1728
48. Huang M, Gao X, Brinson LC (2000) A multivariant micromechanical model for SMAs Part 2. Polycrystal model. Int J Plast 16(10):1371–1390
49. Baxevanis T, Cox A, Lagoudas D (2014) Micromechanics of precipitated near-equiatomic Ni-rich NiTi shape memory alloys. Acta Mech 225(4–5):1167–1185
50. Cox A, Franco B, Wang S, Baxevanis T, Karaman I, Lagoudas D (2017) Predictive modeling of the constitutive response of precipitation hardened Ni-rich NiTi. Shape Mem Superelast 3(1):9–23
51. Joy JK, Solomou A, Baxevanis T, Lagoudas DC (2017) Predicting the constitutive response of precipitation hardened NiTiHf, SPIE smart structures and materials + nondestructive evaluation and health monitoring. In: International society for optics and photonics, pp 101650F-101650F-101659
52. Pun GP, Yamakov V, Mishin Y (2015) Interatomic potential for the ternary Ni–Al–Co system and application to atomistic modeling of the B2–L10 martensitic transformation. Modell Simul Mater Sci Eng 23(6):065006
53. Yamakov V, Hochhalter J, Leser W, Warner J, Newman J, Pun GP, Mishin Y (2016) Multiscale modeling of sensory properties of Co–Ni–Al shape memory particles embedded in an Al metal matrix. J Mater Sci 51(3):1204–1216
54. Tadmor EB, Miller RE (2011) Modeling materials: continuum, atomistic and multiscale techniques. Cambridge University Press, Cambridge
55. Farkas D, Roqueta D, Vilette A, Ternes K (1996) Atomistic simulations in ternary Ni-Ti-Al alloys. Modell Simul Mater Sci Eng 4(4):359
56. Daw MS, Baskes MI (1984) Embedded-atom method: derivation and application to impurities, surfaces, and other defects in metals. Phys Rev B 29(12):6443
57. Foiles S, Baskes M, Daw M (1986) Embedded-atom-method functions for the fcc metals Cu, Ag, Au, Ni, Pd, Pt, and their alloys. Phys Rev B 33(12):7983
58. Lennard-Jones JE (1931) Cohesion. Proc Phys Soc 43(5):461
59. Kastner O (2003) Molecular-dynamics of a 2D model of the shape memory effect. Continuum Mech Thermodyn 15(5):487–502
60. Kastner O (2012) First principles modelling of shape memory alloys: molecular dynamics simulations. Springer, New York
61. Kastner O, Eggeler G, Weiss W, Ackland GJ (2011) Molecular dynamics simulation study of microstructure evolution during cyclic martensitic transformations. J Mech Phys Solids 59(9):1888–1908
62. Lai WS, Liu BX (2000) Lattice stability of some Ni-Ti alloy phases versus their chemical composition and disordering. J Phys 12(5):L53
63. Lai WS, Zhang Q, Liu BX, Ma E (2000) Structural stability and amorphization transition in the Ni–Ti system studied by molecular dynamics simulation with an n-body potential. J Phys Soc Jpn 69(9):2923–2937
64. Mutter D, Nielaba P (2011) Simulation of the thermally induced austenitic phase transition in NiTi nanoparticles. The European Physical Journal B 84(1):109–113
65. Mutter D, Nielaba P (2010) Simulation of structural phase transitions in NiTi. Phys Rev B 82(22):224201
66. Mirzaeifar R, Gall K, Zhu T, Yavari A, DesRoches R (2014) Structural transformations in NiTi shape memory alloy nanowires. J Appl Phys 115(19):194307
67. Yin Q, Wu X, Huang C, Wang X, Wei Y (2015) Atomistic study of temperature and strain rate-dependent phase transformation behaviour of NiTi shape memory alloy under uniaxial compression. Phil Mag 95(23):2491–2512
68. Zhong Y, Gall K, Zhu T (2011) Atomistic study of nanotwins in NiTi shape memory alloys. J Appl Phys 110(3):033532
69. Zhong Y, Gall K, Zhu T (2012) Atomistic characterization of pseudoelasticity and shape memory in NiTi nanopillars. Acta Mater 60(18):6301–6311
70. Ren G, Sehitoglu H (2016) Interatomic potential for the NiTi alloy and its application. Comput Mater Sci 123:19–25
71. Baskes M (1997) Determination of modified embedded atom method parameters for nickel. Mater Chem Phys 50(2):152–158
72. Lee B-J, Baskes M (2000) Second nearest-neighbor modified embedded-atom-method potential. Phys Rev B 62(13):8564
73. Lee B-J, Baskes M, Kim H, Cho YK (2001) Second nearest-neighbor modified embedded atom method potentials for bcc transition metals. Phys Rev B 64(18):184102
74. Ishida H, Hiwatari Y (2007) MD simulation of martensitic transformations in TiNi alloys with MEAM. Mol Simul 33(4–5):459–461
75. Ko W-S, Grabowski B, Neugebauer J (2015) Development and application of a Ni-Ti interatomic potential with high predictive accuracy of the martensitic phase transition. Phys Rev B 92(13):134107

76. Mutter D, Nielaba P (2013) Simulation of the shape memory effect in a NiTi nano model system. J Alloy Compd 577:S83–S87
77. Chowdhury P, Ren G, Sehitoglu H (2015) NiTi superelasticity via atomistic simulations. Philos Mag Lett 95(12):574–586
78. Ko W-S, Maisel SB, Grabowski B, Jeon JB, Neugebauer J (2017) Atomic scale processes of phase transformations in nanocrystalline NiTi shape-memory alloys. Acta Mater 123: 90–101
79. Nam TH, Saburi T (1990) K.i. Shimizu, Cu-content dependence of shape memory characteristics in Ti–Ni–Cu alloys. Mater Trans, JIM 31(11):959–967
80. Nam TH, Saburi T, Nakata Y (1990) K.i. Shimizu, Shape memory characteristics and lattice deformation in Ti–Ni–Cu alloys. Mater Trans, JIM 31(12):1050–1056
81. Frenzel J, Pfetzing J, Neuking K, Eggeler G (2008) On the influence of thermomechanical treatments on the microstructure and phase transformation behavior of Ni–Ti–Fe shape memory alloys. Mater Sci Eng, A 481:635–638
82. Huang X, Ackland GJ, Rabe KM (2003) Crystal structures and shape-memory behaviour of NiTi. Nat Mater 2(5):307–311
83. Hatcher N, Kontsevoi OY, Freeman AJ (2009) Martensitic transformation path of NiTi. Phys Rev B 79(2):020202
84. Vishnu KG, Strachan A (2010) Phase stability and transformations in NiTi from density functional theory calculations. Acta Mater 58(3):745–752
85. Hatcher N, Kontsevoi OY, Freeman AJ (2009) Role of elastic and shear stabilities in the martensitic transformation path of NiTi. Phys Rev B 80(14):144203
86. Morris JR, Ye Y, Krcmar M, Fu CL (2006) The role of phase stability in ductile, ordered B2 intermetallics. In: MRS proceedings, Cambridge Univ Press, pp 0980-II0906-0910
87. Chowdhury P, Patriarca L, Ren G, Sehitoglu H (2016) Molecular dynamics modeling of NiTi superelasticity in presence of nanoprecipitates. Int J Plast 81:152–167
88. Sato T, Saitoh K, Shinke N (2008) Atomistic modelling of reversible phase transformations in Ni–Ti alloys: a molecular dynamics study. Mater Sci Eng, A 481:250–253
89. Khalil-Allafi J, Dlouhy A, Eggeler G (2002) Ni 4 Ti 3-precipitation during aging of NiTi shape memory alloys and its influence on martensitic phase transformations. Acta Mater 50(17):4255–4274
90. Saburi T, Nenno S, Fukuda T (1986) Crystal structure and morphology of the metastable X phase in shape memory Ti-Ni alloys. J Less Common Met 125:157–166
91. Tadaki T, Nakata Y, Shimizu KI, Otsuka K (1986) Crystal structure, composition and morphology of a precipitate in an aged Ti-51 at% Ni shape memory alloy. Trans Jpn Inst Met 27(10):731–740
92. Bataillard L, Bidaux J-E, Gotthardt R (1998) Interaction between microstructure and multiple-step transformation in binary NiTi alloys using in situ transmission electron microscopy observations. Philos Mag A 78(2):327–344
93. Khovailo V, Takagi T, Vasilev A, Miki H, Matsumoto M, Kainuma R (2001) On order–disorder (L21 → B2′) Phase transition in Ni2 + xMn1—xGa heusler alloys. Physica Status Solidi(a) 183(2):R1–R3
94. Brown P, Crangle J, Kanomata T, Matsumoto M, Neumann K, Ouladdiaf B, Ziebeck K (2002) The crystal structure and phase transitions of the magnetic shape memory compound Ni2MnGa. J Phys 14(43):10159
95. Pons J, Santamarta R, Chernenko V, Cesari E (2003) HREM study of different martensitic phases in Ni–Mn–Ga alloys. Mater Chem Phys 81(2):457–459
96. Pons J, Santamarta R, Chernenko VA, Cesari E (2005) Long-period martensitic structures of Ni-Mn-Ga alloys studied by high-resolution transmission electron microscopy. J Appl Phys 97(8):083516
97. Sozinov A, Likhachev A, Lanska N, Söderberg O, Ullakko K, Lindroos V (2004) Stress-and magnetic-field-induced variant rearrangement in Ni–Mn–Ga single crystals with seven-layered martensitic structure. Mater Sci Eng, A 378(1):399–402
98. Enkovaara J (2003) Atomistic simulations of magnetic shape memory alloys. Helsinki University of Technology, Espoo
99. Webster P, Ziebeck K, Town S, Peak M (1984) Magnetic order and phase transformation in Ni2MnGa. Philos Mag B 49(3):295–310
100. Chowdhury P, Sehitoglu H (2016) Significance of slip propensity determination in shape memory alloys. Scripta Mater 119:82–87
101. Holec D, Friák M, Dlouhý A, Neugebauer J (2011) Ab initio study of pressure stabilized NiTi allotropes: pressure-induced transformations and hysteresis loops. Phys Rev B 84(22):224119
102. Chernenko V, Segui C, Cesari E, Pons J, Kokorin V (1998) Sequence of martensitic transformations in Ni-Mn-Ga alloys. Phys Rev B 57(5):2659
103. Segui C, Chernenko V, Pons J, Cesari E, Khovailo V, Takagi T (2005) Low temperature-induced intermartensitic phase transformations in Ni–Mn–Ga single crystal. Acta Mater 53(1):111–120
104. Kimiecik M, Jones JW, Daly S (2016) The effect of microstructure on stress-induced martensitic transformation under cyclic loading in the SMA Nickel-Titanium. J Mech Phys Solids 89:16–30
105. Yawny A, Sade M, Eggeler G (2005) Pseudoelastic cycling of ultra-fine-grained NiTi shape-memory wires. Zeitschrift für metallkunde 96(6):608–618
106. Eucken S, Duerig TW (1989) The effects of pseudoelastic prestraining on the tensile behaviour and two-way shape memory effect in aged NiTi. Acta Metall 37(8):2245–2252
107. Chowdhury PB (2016) Modeling mechanical properties–linking atomistics to continuum. University of Illinois at Urbana-Champaign, Urbana
108. Chowdhury P, Sehitoglu H (2018) Atomistic energetics and critical twinning stress prediction in face and body centered cubic metals: recent progress. J Eng Mater Technol 140(2): 020801
109. Chowdhury P, Sehitoglu H, Abuzaid W, Maier H (2015) Mechanical response of low stacking fault energy Co–Ni alloys–Continuum, mesoscopic and atomic level treatments. Int J Plast 71:32–61
110. Chowdhury P, Sehitoglu H, Maier H, Rateick R (2016) Strength prediction in NiCo alloys–the role of composition and nanotwins. Int J Plast 79:237–258
111. Suresh S (1998) Fatigue of materials. Cambridge University Press, Cambridge
112. Chowdhury P, Sehitoglu H (2016) Mechanisms of fatigue crack growth–a critical digest of theoretical developments. Fatigue Fract Eng Mater Struct 39(6):652–674
113. Eggeler G, Hornbogen E, Yawny A, Heckmann A, Wagner M (2004) Structural and functional fatigue of NiTi shape memory alloys. Mater Sci Eng, A 378(1):24–33
114. Sedmák P, Šittner P, Pilch J, Curfs C (2015) Instability of cyclic superelastic deformation of NiTi investigated by synchrotron X-ray diffraction. Acta Mater 94:257–270
115. Pelton A (2011) Nitinol fatigue: a review of microstructures and mechanisms. J Mater Eng Perform 20(4–5):613–617
116. Chowdhury P, Sehitoglu H, Rateick R (2018) Damage tolerance of carbon-carbon composites in aerospace application. Carbon 126:382–393

117. Horstemeyer M, Farkas D, Kim S, Tang T, Potirniche G (2010) Nanostructurally small cracks (NSC): a review on atomistic modeling of fatigue. Int J Fatigue 32(9):1473–1502
118. Potirniche G, Horstemeyer M, Gullett P, Jelinek B (2006) Atomistic modelling of fatigue crack growth and dislocation structuring in FCC crystals. In: Proceedings of the Royal Society of London A: mathematical, physical and engineering sciences, The Royal Society, pp 3707–3731
119. Tang T, Kim S, Horstemeyer M (2010) Fatigue crack growth in magnesium single crystals under cyclic loading: molecular dynamics simulation. Comput Mater Sci 48(2):426–439
120. Baker KL, Warner D (2014) An atomistic investigation into the nature of near threshold fatigue crack growth in aluminum alloys. Eng Fract Mech 115:111–121
121. Zamora R, Baker K, Warner D (2015) Illuminating the chemo-mechanics of hydrogen enhanced fatigue crack growth in aluminum alloys. Acta Mater 100:232–239
122. Chowdhury PB, Sehitoglu H, Rateick RG, Maier HJ (2013) Modeling fatigue crack growth resistance of nanocrystalline alloys. Acta Mater 61(7):2531–2547
123. Chowdhury PB, Sehitoglu H, Rateick RG (2014) Predicting fatigue resistance of nano-twinned materials: part I-Role of cyclic slip irreversibility and Peierls stress. Int J Fatigue 68:277–291
124. Chowdhury PB, Sehitoglu H, Rateick RG (2014) Predicting fatigue resistance of nano-twinned materials: part II–Effective threshold stress intensity factor range. Int J Fatigue 68:292–301
125. Chowdhury P (2011) Fatigue crack growth (FCG) modeling in the presence of nano-obstacles. University of Illinois at Urbana-Champaign, Urbana
126. Alkan S, Chowdhury P, Sehitoglu H, Rateick RG, Maier HJ (2016) Role of nanotwins on fatigue crack growth resistance–Experiments and theory. Int J Fatigue 84:28–39
127. Niemann R, Rößler UK, Gruner ME, Heczko O, Schultz L, Fähler S (2012) The role of adaptive martensite in magnetic shape memory alloys. Adv Eng Mater 14(8):562–581
128. Entel P, Siewert M, Gruner ME, Herper HC, Comtesse D, Arróyave R, Singh N, Talapatra A, Sokolovskiy VV, Buchelnikov VD (2013) Complex magnetic ordering as a driving mechanism of multifunctional properties of Heusler alloys from first principles. Eur Phys J B 86(2):1–11
129. Chowdhury P, Sehitoglu H, Rateick R (2016) Recent advances in modeling fatigue cracks at microscale in the presence of high density coherent twin interfaces. Curr Opin Solid State Mater Sci 20(3):140–150